Design and optimization of lattice structures for aerospace applications

Enrico Stragiotti

François-Xavier Irisarri[1], Cédric Julien[1] and Joseph Morlier[2]

1: ONERA - The French Aerospace Lab
DMAS - Département matériaux et structures
92320 Châtillon, France
{francois-xavier.irisarri, cedric.julien}@onera.fr

2: ICA - Institut Clément Ader
ISAE - SUPAERO
31400 Toulouse, France
joseph.morlier@isae-supaero.fr

January 21, 2024

PhD manuscript

ONERA – ISAE Supaero

Colophon
This document was typeset with the help of KOMA-Script and LaTeX using the kaobook class.

ONERA – ISAE Supaero

Contents

Contents iii

List of Figures v

List of Tables v

List of Abbreviations v

Abstract 1

Introduction 3

Conclusion and perspectives 7

Appendix 13

A. Sensitivity analysis of the modular structure optimization algorithm 15
- A.1. Optimization formulation, objective function and constraints . . . 15
- A.2. Common derivatives . . . 16
- A.3. Gradient . . . 17
- A.4. Jacobian matrix . . . 17
- A.5. Hessian matrix . . . 19

Bibliography 21

List of Figures

1. (a) The transonic truss-braced wing called ALBATROS by ONERA [1, 2]; (b) the Blended-Wing Body (BWB) zero-e demonstrator by Airbus [3]. 3
2. [5] [6]. 4

List of Tables

A.1. Reminder of the indexes used for the sensitivity analysis of the layout and topology optimization of modular structures. 15

List of Abbreviations

BWB	Blended-Wing Body
CRM	NASA Common Research Model
DMO	Discrete Material Optimization
DOE	Design of experiments
FEA	Finite Element Analysis
RAMP	Rational Approximation of Material Properties
TTO	Truss Topology Optimization

Abstract

todo

Introduction

Scientists study the world as it is,
Engineers create the world that never has been.

— Theodore von Kármán

Towards lighter structures

In the aerospace industry, an ongoing demand exists for lighter aerostructures, motivated by the need to enhance fuel efficiency and overall performance. This emphasis on lighter structures and materials not only reduces operational costs for airlines but also aligns with a broader commitment to sustainability, mitigating fuel consumption and carbon emissions. Furthermore, the aerospace sector is currently witnessing two innovative shifts: the transition to hydrogen-powered and electric planes, directing engineering efforts toward cleaner and more sustainable aviation technologies. These changes offer opportunities to deviate from the classic tube-and-wing configuration and explore inventive concepts like the flying wing Blended-Wing Body (BWB), in which the fuselage and the wing blend together to form an aircraft in which the fuselage, widened and integrated into the wing, also contributes significantly to the lift, or transonic truss-braced wings, with the goal of direct reduction in the aerodynamic drag by using a high-aspect ratio strut-braced wing configuration (see examples in Fig. 1). Regardless of the specific configuration, a highly probable shared goal is the necessity to redesign lightweight dry–i.e. with no fuel tanks inside–wings with high aspect ratios and thin profiles.

(a)

(b)

Figure 1.: (a) The transonic truss-braced wing called ALBATROS by ONERA [1, 2]; (b) the Blended-Wing Body (BWB) zero-e demonstrator by Airbus [3].

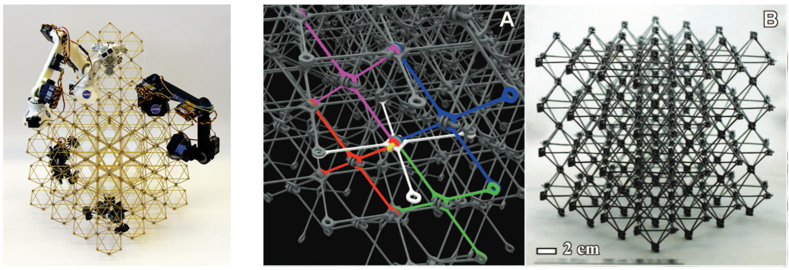

(a) (b)

Figure 2.: [5] [6].

To meet these criteria, a promising solution involves the application of lattice structures. Not only do these structures provide the necessary ultralight properties, but they also offer modularity. Modular designs come with several advantages, notably the capability to construct large structures using smaller, more easily manufactured repeating modules. Other notable properties include on-field reparability, improved damage resistance, fast assembly for temporary structures, and stochastic error detection and repair compared to conventional monolithic material systems [4]. Additionally, recent research opens up the possibility of a fully robotic assembly phase, permitting faster and more reliable assembly (see Fig. 2).

4. Belvin et al. (2016), 'In-Space Structural Assembly'

Optimizing lattice structures involves four main dimensions: material, module shape, layout, and topology. Material optimization focuses on improving mechanical properties by tailoring the distribution of lattice constituents, while shape optimization fine-tunes individual module external geometries. Layout optimization arranges modules in space, defining their presence or absence, and topology optimization refines overall arrangement and connections within each module. Navigating these dimensions enables engineers to tailor lattice structures for a balance between weight, strength, and functionality. However, the abundance of design choices poses a significant challenge due to the lack of a standardized design method. Navigating this intricate landscape requires a systematic and efficient approach to ensure the resulting lattice structure meets specific engineering requirements.

Objective

This thesis aims to develop an optimization formulation and algorithm specifically designed for ultralight and modular aerostructures within the aerospace industry. In this field, reducing weight is crucial for improving overall performance. However, the introduction of modularity, while offering advantages such as manufacturing easing or improved damage resistance, may potentially lead to an increase in the overall weight of the structure when compared to classic monolithic structures. Consequently, the primary objective throughout this thesis is to develop an optimization method that not only harnesses the benefits of modularity but also ensures that the resultant structure remains as lightweight as possible. Striking a balance between the manufacturing advantages conferred by modularity and the critical need for weight reduction forms the central focus of this research.

Outline of the thesis

The remainder of the thesis is structured as follows. Chapter **??** provides a comprehensive review of structural optimization algorithms, especially focusing on ultralight weight and modular cases. The chapter introduces density-based topology optimization and the Truss Topology Optimization (TTO) formulations that will be utilized throughout the document. Chapter **??** delves into a detailed comparison of the topology optimization methods, emphasizing results obtained when optimized structures exhibit a very low volume fraction, i.e. less than 5 %. A shared volume minimization with stress constraints formulation is presented, and a comparison is conducted by varying the material mechanical properties to achieve different volume fractions. After careful analysis, the TTO approach is selected due to its reduced computational time and suitability for modeling lightweight structures. Chapter **??** addresses the limitations of the classic TTO formulation, such as the absence of local buckling constraints, minimum slenderness limits, consideration of multiple load cases, and ensuring mechanical compatibility for complex structures. To overcome these challenges, an innovative volume minimization formulation is proposed, incorporating the additional constraints needed to optimize real-world structures. Due to the inherent multimodality of the formulation, a two-step optimization algorithm is introduced, utilizing a relaxed problem to generate an initial approximate solution for subsequent optimization using a complete formulation. The Reinitialization heuristic is also proposed to reduce the influence of the starting point on optimization results. Chapter **??** explores the incorporation of modular constraints in the proposed TTO formulation, employing the full-scale variable linking approach. This approach repeats a single module throughout the entire design to create optimized modular structures. The chapter evaluates the impact of hyperparameters, such as the number of subdomains and module complexity, on the mechanical performance of the structure. A Design of Experiments (Design of experiments (DOE)) based on the chapter's results provides guidance on choosing hyperparameters for optimization. In Chapter **??**, the optimization scenario becomes more complex by introducing an additional optimization variable: the addition of multiple different topology modules. This optimization, inherently more complex, involves optimizing not only the modules' topology but also the layout of the modules within the structure. A modified Discrete Material Optimization (DMO) approach is employed, utilizing a gradient-based optimizer, while the starting point is determined by employing k-means clustering on the stress distribution of the unoptimized initial structure. Up to this point, the focus has been on academic two or three-dimensional test cases. Chapter Chapter **??** extends the application of the proposed optimization formulation and algorithms to the aerospace domain. Initially, the monolithic optimization algorithm is used to reduce the weight of the wingbox of the NASA Common Research Model (CRM), a standard benchmark for aeronautic research. The test case is subjected to multiple load cases(+2.5g, -1g and cruise loads) associated with some correspective safety factors. The optimization is conducted using different materials and discretizations, resulting in lighter structures in less time compared to the literature. Later, the modular optimization formulation presented in Chapter **??** is used on a drone-sized wing based on the 0012 NACA wing profile. Additionally, follow-up scientific perspectives are discussed.

Conclusion and perspectives

Conclusion

In the aerospace sector the reduction of weight plays a fundamental role, due to the high interdependency between weight and lift. In aviation, reducing aircraft weight is crucial because it lowers the wing loading, improving aerodynamic efficiency, maneuverability, and fuel efficiency. This is because not only is an economic concerm but more and more an environmental defis. to answer to tese defis, new concepts such the flying wing or the use of transonic truss braced wings with high elongation have been proposed. a shared need of these concepts is to use thin dry wings with high aspect ratio. A possible design concept that could fitt well in this context is to use lattice structures as primary structure of these wings, thanks to their inherent low mass and all the benefit of a modular costruction. The problem with this concept is that there is a lack of standardized method to design and optimize them. For all of these reason, this thesis presented the developement of a design method and an optimization algorithm for ultralight lattice structures.

In Chapter **??** we conduted a throughtful comparison between two of the most pertinent optimization framework for optimizing ultrlight structures: the density based topology optimization and the TTO approaches. First, a shared volume minimization with material resistance constraints formulation is developed for both methods. Then, after having explored the modelizationdifference of the two approaches–expecially the difference between nand and sand approaches, a series of numerical test have been performed using the two dimensional l shaped beam as test case. To obtain different values of volume fraction of the optimized structure, we modified gradually the material properties–i.e. a high value of strenght is associated witha low volume fraction–. We tracked for every test the volume fraction, the compliance, the material resistance and the comutational time, and we discovered principally two limits in the range of applicability of the two methods: the density based topology optimization approaches inevitably reaches a limit at low volume fractions as the continuous discretization needs a continuous refinelment to go to low fractions. This greatly adds to the comutational cost of the optimization, as not only the Finite Element Analysis (FEA) takes longer, but also because the number cof design variables and sensityvity analysis is concerded. On the other hands, the TTO deos not show this problem, but it have a diametral problem: if we go towards very high volume fractions the radius of the cross sectional areas is too big and the truss idealization lose sense. Concerning the comutational time, we have observed that the tto approach, thanks to being linear, permits a. a last important difference is that with a continuous discretization more elements are needed if we want to have more detials in the opptimized structure, while if we are using tto with a ground structure discretization, this is true no more. Thanks to all these observations, we decided to carry on the work on TTO as it is fitting really well our idea to work on ultralight structures.

Now that the choiche to use tto is done, in chapter 3 we want to address the main limitations of this method and to improve the applicability. First, we concieved a constraint on the minimu slenderness of the active bars of the optimized structures, tring to stretch the domain of applicability of the method. Later, we interessed on the addition of local buckling constraints to the problem, indispensabile for very lighweight structures. special attention was needed in this case as we wanted to solve the broblem of nodal stability of copressed bars– referred as buckling chains or topological buckling in the literature–. Finally, we modeled kinematic compatibility constraints, needed to treat more complex problems that results in a statically inadmissible structure– such in the case of using multiple load cases or imposed symmeties–. We formulated then the full tto formulation with all these addition, taht could be solved also for multiple load cases. We observed, however that naively implementing this formulation on an NLP solver was unsuccesfull– i.e. the solution was presentin always a lot of candidates, the optimizer was uncapable of discerning which bar should be active in the solution–, as the problem is extremely multimodal and it was not capable of dealing with all of these contraints contemporaneamente. For that reason we developed an innovtive two step optimimization algorithm, utilizing a relaxed problem to generate an initial approximate solution for subsequent optimization using a complete formulation. The Reinitialization heuristic is also proposed to reduce the influence of the starting point on optimization results. thanks to that, we were able to show how the proposed algorithm is capable of efficacely dealing with some problems of the literature, as the ten-bar truss, where we showed zero influence of the starting point with 100 random initializations, or to find better solution to the 2D cantilever beam problem proposed by Achzingher. Finally we tested the proposed algorithm on more complex load cases, suc as a two dimensional truss with multiple load cases, showing the necessity to add kinematic constraints to the formulation, and to optimize a three dimensional strucure, showing the versatility of the formulation.

In Chapter **??** we interest in how to implement modular constraints in the proposed TTO formulation. We decided to use a full-scale method–so a methodh that does not assume pysical scale separation between the module and the whole strucute– called variable linking, in which the periodicity of the structure is created by linking the design variables of different subdomains of the structure. We improved this method by permitting to consider multiple modules' topology mathematically modeling this using the Kronecher product. In the following part of the chapter we put the formulation to the test by running a multitude of different numercial optimization in order to explore the limit and the trends of the modular tto optimization. First, we showed how closely related are multi moad cases and modular structures, underlying then the need for kinematic compatibility constraints for modular structurres. Then, we performed a parametric study on two hyperparameters of the modular optimization: the number of subdomains and the complexity of the module–i.e. the number of candidates used to discretize a module. Using the numerical results of this test we constructed a Design of experiments (DOE), we provided some recommendations based on that: fewer subdomains are generally preferable, with the module as large as manufacturably possible. Module complexity plays a role in volume minimization but has a relatively low impact. Finally, the modular TTO structures are benchmarked against one of the most commonly used module topologies in the literature: the octet-truss lattice.

The modular results obtained till now showed an increased volume when compared to the correspective monolitich structure. This increase in mass is expected as we are repeating the same module over and over the design space, where there could be different loading consitions. the module is then obliged to show mechainical properties that works well everywhere in the structure. Trying to reduce the gap between modular and monolitic structures, in Chapter **??** we added a new design variable to the problem: the layout of the modules in the space. The problem is then retrasformed in the following: we optimize the topology of multiple modules and concurrently we dispose then in the design domain. This problem is extremely more difficoult as there exist a strong connexion between the module topology and the layout, and due to the fact that the layout of the modules is inherently a discrete problem. The discrete design space is firstly relaxed using a continuous modelization and on which we used a modified DMO approach, utilizing a gradient-based optimizer. To reduce the risk of converging towards non-pysical solutions– such as solutions that presents a mix of modules topologies– we developed a dual penalization scheme based on the RAMP method. Finding an appropriate starting point for the optimization proved to be non-trivial, as the topology of the modules is closely tied with the module layout, and vice versa. We employed the k-means clustering approch on the stress distribution of the unoptimized initial structure to provide a first module layput for the problem. THe proposed formulation is tested against multiple two and three dimensional test cases, finding better results than the literature. finally we showed how the control of the number of module topologies and the control on the presence or not of a subdomain is an effective ways to reduce the gab between monolitich and modular structures, all while maintaining the modular advntages. It is important however to remind that having more modules is tied with higher mnufacturing complexity. It will be then the user to decide the best fit value for the required application.

Up untill this poijnt, we presented only academic test cases. In Chapter **??** we deal with two apllications taken from the aerospace domain. Initially, the monolithic optimization algorithm is used to reduce the weight of the wingbox of the CRM, a standard benchmark for aeronautic research. The test case is subjected to multiple load cases(+2.5g, -1g and cruise loads) associated with some correspective safety factors. The optimization is conducted using different materials and discretizations, resulting in lighter structures in less time compared to the literature. Later, the modular optimization formulation presented in Chapter **??** is used on a drone-sized wing based on the 0012 NACA wing profile, showing how the proposed algorithm can be applied to complex real-world scenario test cses.

Perspectives

The possibilities offered by this research are manifold. Some part concerns the methodology directly, with research directions which were not explored, and others are about the future possibilities. we will review here a list of the possible perspectives grouped by chapter.

In Chapter **??** we only deal with generic density based topology optimization. It would have been interesting to see how the results would change if we compared to . We speculte, however, that as these methods still relies on the continuous discretization for the fea and for the sensitivity analysis, the results should not be too different from what we presented, expecially when comparing the computational time.

Considering the Chapter **??**, we have dealed principally with local buckling constraints, but it would definetly be interesting ipmelemnt gobal buckling contraints as well. Then, we used always bar elements and not beam elements, negleting the influence of the joint stiffness in the optimization. We know that these assumptions hold for high value of slenderness, but it would be interesting to see what it happens if we make this swithc. Lastly, we added essentially multiple mechanical contratins to the optimization and the manufacturing complexity is discussed here only as an outcome of the optimization strategy. However, it would be important to consider additional manufacturing constarints (maximum numbers of bars converging to a single node, minimum section, imposed periodicity of the structure) during the optimization would be beneficial.

In Chapter **??** we always considered cubic modules. However, the module external shape–as the ratio between the dimensions or the shape that could be pyramidal or dodecaedric– has cenrtantly a big influence on the mechainical properties of the module itself. THis additional design variable of the modular problem should be investigated, balancing the tradeoff betweeen shape complexity, mass, and manufacturing complexity. It should be noted that thre exists multiple studies on the tassellation of 2d and 3d space, and these studies could be a good inspiration for working in this direction. Additionally, we have only considered the study of topological buckling inside the module, while it would be interesting study how to algorithmically implement topological buckling at the structure level.

Chapter **??** ha messo in luce the big sfida in concurrently optimizing the modules' topology and layout. Even if the proposed pertubation of the starting point proved to work well in addressing this problem, a more complex heuristic could be beneficial for the optimization. One could for example solve an alternating formulation in wich first we optimize the layout and then the topology in a repetitive manner till convergence instead of the complex concuren optimization.

Finally, in Chapter **??** we obseerved how important the choice of the initial ground strucutre is fo the optimization of real sized structures. Major studies should be conducted on how to concieve the best ground sructure for a specific problem.

Appendix

A Sensitivity analysis of the modular structure optimization algorithm

In this appendix, we demonstrate how the gradient, Jacobian, and Hessian matrices of the objective function and the optimization constraints are evaluated for the layout and topology optimization formulation $\mathbb{M}_2$ presented in Chapter **??**. This step, called sensitivity analysis, is crucial for gradient descent optimization algorithms, as it allows for faster and more accurate convergence compared to using finite differences. We remind the reader that the index i is relative to the number of bars in a module $\bar{n}$, the index j is relative to the number of subdomains N_{sub} in which the structure is divided, and the index t is relative to the number of different modules' topologies N_{T}. The indexes are summarized in Table A.1 for added clarity.

More information on sensitivity analysis can be found in the book by Martins and Ning [7].

Index	Interval	Expl.
i	$[0, \bar{n}[$	# of bars in a module
j	$[0, N_{\text{sub}}[$	# of sub-domains
t	$[0, N_{\text{T}}[$	# of modules' topologies

Table A.1.: Reminder of the indexes used for the sensitivity analysis of the layout and topology optimization of modular structures.

A.1. Optimization formulation, objective function and constraints

The relaxed formulation $\mathbb{M}_2$ for which we want to perform the sensitivity analysis is expressed in terms of modules' cross-sectional area $\bar{\boldsymbol{a}}$, module selection variables $\boldsymbol{\alpha}$, and member forces $\boldsymbol{q}$ as:

$$\begin{aligned}
\min_{\bar{\boldsymbol{a}},\boldsymbol{\alpha},\boldsymbol{q}} \quad & V = \sum_{j=1}^{N_{\text{sub}}} \bar{\boldsymbol{\ell}}^T \tilde{\boldsymbol{a}}^j && \text{(Volume minimization)} \\
\text{s.t.} \quad & \boldsymbol{B}\boldsymbol{q} = \boldsymbol{f} && (g_{\text{eq}}) \\
& \boldsymbol{q} \geq -\frac{\boldsymbol{s}\boldsymbol{a}^2}{\boldsymbol{\ell}^2} && (g_{\text{buck}}) \\
& -\sigma_C \boldsymbol{a} \leq \boldsymbol{q} \leq \sigma_T \boldsymbol{a} && (g_{\text{st,t}},\ g_{\text{st,c}}) \\
& 0 \leq \bar{\boldsymbol{a}} \leq \frac{4\pi\bar{\boldsymbol{\ell}}^2}{\lambda_{\max}} && (g_{\text{slend}}) \\
& \sum_{t=1}^{N_{\text{T}}} \alpha_t^j \leq 1,\ \forall j && (g_{\text{sum}}),
\end{aligned} \tag{$\mathbb{M}_2$}$$

in which

$$V = \sum_{j=1}^{N_{\text{sub}}} \bar{\boldsymbol{\ell}}^T \tilde{\boldsymbol{a}}^j, \tag{A.1}$$

represents the structural volume of the modular structure and acts as the objective function to minimize for the optimization. The vector $\tilde{\boldsymbol{a}}^j$, representing the increased cross-sectional areas of the j-th subdomain, is defined as follows:

$$\tilde{\boldsymbol{a}}^j = \sum_{t=1}^{N_{\text{T}}} \tilde{w}_t^j \bar{\boldsymbol{a}}_t, \tag{A.2}$$

and where $\tilde{w}$ is evaluated using the Rational Approximation of Material Properties (RAMP) interpolation scheme with the q parameter as follows:

$$\tilde{w}_t^j = \frac{\alpha_t^j}{1 + q(1 - \alpha_t^j)}. \tag{A.3}$$

The cross-sectional areas vector $\boldsymbol{a}^j$ of subdomain j used for the constraints evaluation is expressed as:

$$\boldsymbol{a}^j = \sum_{t=1}^{N_{\mathrm{T}}} w_t^j \bar{\boldsymbol{a}}_t, \tag{A.4}$$

where $\bar{\boldsymbol{a}}_t$ represent the vector of cross-sectional areas of the t module and $\boldsymbol{w}^j$ is the vector of weight relatives to the j subdomain, defined as $\boldsymbol{w}^j \in \mathbb{R}^t \,|\, w_j^t \in [0,1]$. Its relationship with the weight w is as follows:

$$w_t^j = \frac{\alpha_t^j}{1 + p(1 - \alpha_t^j)}, \tag{A.5}$$

where $p \in \mathbb{R}^+$ denotes a parameter governing the steepness of the RAMP interpolation.

A.2. Common derivatives

We introduce here some important derivatives that we use all along the Chapter.

$$\frac{\partial \boldsymbol{a}^j}{\partial \bar{\boldsymbol{a}}_t} = w_t^j, \tag{A.6}$$

$$\frac{\partial \boldsymbol{a}^j}{\partial \alpha_t^j} = \frac{\partial \boldsymbol{a}^j}{\partial w_t^j} \frac{\partial w_t^j}{\partial \alpha_t^j}, \tag{A.7}$$

where

$$\frac{\partial \boldsymbol{a}^j}{\partial w_t^j} = \bar{\boldsymbol{a}}_t, \tag{A.8}$$

and

$$\frac{\partial w_t^j}{\partial \alpha_t^j} = \frac{1 + (\cdot)}{\left(1 + (\cdot)(1 - \alpha_t^j)\right)^2}, \tag{A.9}$$

where $(\cdot)$ is either equal to p or q.

$$\frac{\partial^2 w_t^j}{\partial (\alpha_t^j)^2} = \frac{2(\cdot)\,(1 + (\cdot))}{\left(1 + (\cdot)(1 - \alpha_t^j)\right)^3}. \tag{A.10}$$

A.3. Gradient

The gradient of the objective function V is non-zero only for the design variables $\bar{\boldsymbol{a}}$ and $\boldsymbol{\alpha}$. It is evalued for $\bar{\boldsymbol{a}}$ as following:

$$\frac{\partial V}{\partial \bar{\boldsymbol{a}}_t} = \bar{\boldsymbol{\ell}}^T \sum_{j=1}^{N_{\text{sub}}} \tilde{w}_t^j, \text{ with } t \in [1, \dots, N_T]. \tag{A.11}$$

The gradient with respect to $\boldsymbol{\alpha}$ can be written as:

$$\frac{\partial V}{\partial \alpha_t^j} = \frac{\partial V}{\partial w_t^j} \frac{\partial w_t^j}{\partial \alpha_t^j}, \tag{A.12}$$

where

$$\frac{\partial V}{\partial w_t^j} = \bar{\ell}^T \bar{\boldsymbol{a}}_t, \tag{A.13}$$

and evalued using Equation A.9 and the parameter q. As already mentioned, the gradient is zero with respect to the member forces $\boldsymbol{q}$:

$$\frac{\partial V}{\partial \boldsymbol{q}} = 0. \tag{A.14}$$

A.4. Jacobian matrix

We focus now on the evaluation of the Jacobian matrix of the optimization constraints with respect to the design variables.

Equilibrium constraints The equilibrium constraint g_{eq} is linear on $\boldsymbol{q}$ and not dependent on $\bar{\boldsymbol{a}}$ and $\boldsymbol{\alpha}$. For that reason we can write:

$$\frac{\partial g_{\text{eq}}}{\partial \bar{\boldsymbol{a}}} = 0, \tag{A.15}$$

$$\frac{\partial g_{\text{eq}}}{\partial \boldsymbol{\alpha}} = 0, \tag{A.16}$$

$$\frac{\partial g_{\text{eq}}}{\partial \boldsymbol{q}} = \boldsymbol{B}. \tag{A.17}$$

Stress constraints Knowing that:

$$\frac{\partial g_{\text{st,t}}^j}{\partial \boldsymbol{a}^j} = -\sigma_t, \tag{A.18}$$

and

$$\frac{\partial g_{\text{st,c}}^j}{\partial \boldsymbol{a}^j} = \sigma_c, \tag{A.19}$$

the Jacobian for the stress constraints $g_{\text{st,t}}$ and $g_{\text{st,c}}$ can be evalued using Equation A.6 and Equation A.7 as follows:

$$\frac{\partial g^j_{\text{st},*}}{\partial \bar{\boldsymbol{a}}_t} = \frac{\partial g^j_{\text{st},*}}{\partial \boldsymbol{a}^j} \frac{\partial \boldsymbol{a}^j}{\partial \bar{\boldsymbol{a}}_t}, \tag{A.20}$$

and

$$\frac{\partial g^j_{\text{st},*}}{\partial \alpha^j} = \frac{\partial g^j_{\text{st},*}}{\partial \boldsymbol{a}^j} \frac{\partial \boldsymbol{a}^j}{\partial \alpha^j}, \tag{A.21}$$

where the asterisk $*$ refers to either the compression and the tension constraints. The stress constraints are linear with respect to q:

$$\frac{\partial g_{\text{st},*}}{\partial \boldsymbol{q}} = \mathbf{1}, \tag{A.22}$$

in which $\mathbf{1}$ represent a vector of all ones.

Buckling constraints Knowing that:

$$\frac{\partial g^j_{\text{buck}}}{\partial \boldsymbol{a}^j} = 2\frac{s\,\boldsymbol{a}^j}{\boldsymbol{\ell}^2}, \tag{A.23}$$

the Jacobian for the buckling constraints g_{buck} with respect to $\bar{\boldsymbol{a}}$ can be evalued using Equation A.6 as:

$$\frac{\partial g^j_{\text{buck}}}{\partial \bar{\boldsymbol{a}}_t} = \frac{\partial g^j_{\text{buck}}}{\partial \boldsymbol{a}^j} \frac{\partial \boldsymbol{a}^j}{\partial \bar{\boldsymbol{a}}_t}. \tag{A.24}$$

Using Equation A.7 we evaluate the derivative with respect to $\boldsymbol{\alpha}$ as:

$$\frac{\partial g^j_{\text{buck}}}{\partial \alpha^j} = \frac{\partial g^j_{\text{buck}}}{\partial \boldsymbol{a}^j} \frac{\partial \boldsymbol{a}^j}{\partial \alpha^j}. \tag{A.25}$$

Maximum sum alpha constraints The constraint g_{sum} on the maximal value of α in every subdomain is linear with respect to α and it does not depend on the other design variables. For that reason we can write:

$$\frac{\partial g_{\text{sum}}}{\partial \bar{\boldsymbol{a}}} = 0, \tag{A.26}$$

$$\frac{\partial g_{\text{sum}}}{\partial \boldsymbol{\alpha}} = \mathbf{1}, \tag{A.27}$$

$$\frac{\partial g_{\text{sum}}}{\partial \boldsymbol{q}} = 0. \tag{A.28}$$

A.5. Hessian matrix

For the evaluation of the hessian matrix, we list here only the nonzero contributions, assuming that all the remaining are zero.

Volume The only nonzero contributions to the Hessian matrix are:

$$\frac{\partial^2 V}{\partial \bar{\boldsymbol{a}}_t \partial \alpha_t^j} = \bar{\ell}^T \frac{\partial \tilde{w}_t^j}{\partial \alpha_t^j}, \tag{A.29}$$

and

$$\frac{\partial^2 V}{\partial (\alpha_t^j)^2} = \bar{\ell}^T \bar{\boldsymbol{a}}_t \frac{\partial^2 w_t^j}{\partial (\alpha_t^j)^2}, \tag{A.30}$$

that can be evaluated using Equation A.9 and Equation A.10

Equilibrium constraints All terms are zero for the equilibrium constraints.

Stress constraints

$$\frac{\partial^2 g_{\mathrm{t}}^j}{\partial \bar{\boldsymbol{a}}_t \partial \alpha_t^j} = -\sigma_t \frac{\partial w_t^j}{\partial \alpha_t^j}, \tag{A.31}$$

$$\frac{\partial^2 g_{\mathrm{t}}^j}{\partial (\alpha_t^j)^2} = -\sigma_t \bar{\boldsymbol{a}}_t \frac{\partial^2 w_t^j}{\partial (\alpha_t^j)^2}. \tag{A.32}$$

Buckling constraints To evaluate the Hessian of buckling constraints we need to define two additional indexes, l and m that are spanning from 0 to $N_{\mathrm{T}} - 1$ as the index t. We can then write:

$$\frac{\partial^2 g_{\mathrm{buck}}^j}{\partial \bar{\boldsymbol{a}}_l \partial \bar{\boldsymbol{a}}_m} = 2 \frac{s}{\boldsymbol{\ell}^2} w_l^j w_m^j. \tag{A.33}$$

The mixed term is evaluated as follow:

$$\frac{\partial^2 g_{\mathrm{buck}}^j}{\partial \bar{\boldsymbol{a}}_l \partial \alpha_m^j} = 2 \frac{s}{\boldsymbol{\ell}^2} w_l^j \frac{\partial \boldsymbol{a}^j}{\partial \alpha_m^j} + 2 \frac{s\,\boldsymbol{a}^j}{\boldsymbol{\ell}^2} \frac{\partial w_l^j}{\partial \alpha_m^j}, \tag{A.34}$$

$$\frac{\partial^2 g_{\mathrm{buck}}^j}{\partial \bar{\boldsymbol{a}}_l \partial \alpha_m^j} = 2 \frac{s}{\boldsymbol{\ell}^2} w_l^j \frac{\partial w_m^j}{\partial \alpha_m^j} \bar{\boldsymbol{a}}_m + 2 \frac{s\,\boldsymbol{a}^j}{\boldsymbol{\ell}^2} \frac{\partial w_l^j}{\partial \alpha_m^j}, \tag{A.35}$$

$$\frac{\partial^2 g_{\mathrm{buck}}^j}{\partial \bar{\boldsymbol{a}}_l \partial \alpha_m^j} = \begin{cases} 2 \frac{s}{\boldsymbol{\ell}^2} \frac{\partial w_t^j}{\partial \alpha_t^j} \left(w_t^j \bar{\boldsymbol{a}}_t + \boldsymbol{a}^j \right) & \text{if } l = m = t \\ 2 \frac{s}{\boldsymbol{\ell}^2} w_l^j \frac{\partial w_m^j}{\partial \alpha_m^j} \bar{\boldsymbol{a}}_m & \text{otherwise.} \end{cases} \tag{A.36}$$

And finally the quadratic term in α:

$$\frac{\partial^2 g^j_{\text{buck}}}{\partial \alpha^j_l \partial \alpha^j_m} = 2\frac{s}{\boldsymbol{\ell}^2}\bar{\boldsymbol{a}}_l \frac{\partial \boldsymbol{a}^j}{\partial \alpha^j_m}\frac{\partial w^j_l}{\partial \alpha^j_l} + 2\frac{s\,\boldsymbol{a}^j}{\boldsymbol{\ell}^2}\bar{\boldsymbol{a}}_l \frac{\partial^2 w^j_l}{\partial \alpha^j_l \partial \alpha^j_m}, \tag{A.37}$$

$$\frac{\partial^2 g^j_{\text{buck}}}{\partial \alpha^j_l \partial \alpha^j_m} = \begin{cases} 2\frac{s}{\boldsymbol{\ell}^2}\bar{\boldsymbol{a}}_t^2 \left(\frac{\partial w^j_t}{\partial \alpha^j_t}\right)^2 + 2\frac{s\,\boldsymbol{a}^j}{\boldsymbol{\ell}^2}\bar{\boldsymbol{a}}_t \frac{\partial^2 w^j_t}{\partial (\alpha^j_t)^2} & \text{if } l = m = t \\ 2\frac{s}{\boldsymbol{\ell}^2}\bar{\boldsymbol{a}}_l \bar{\boldsymbol{a}}_m \left(\frac{\partial w^j_m}{\partial \alpha^j_m}\right)\left(\frac{\partial w^j_l}{\partial \alpha^j_l}\right) & \text{otherwise.} \end{cases} \tag{A.38}$$

Maximum sum alpha constraints All terms are zero for the g_{sum} constraint.

Bibliography

[1] Carrier, G., Atinault, O., Dequand, S., and Toussaint, C., 'Investigation of a Strut-Braced Wing Configuration for Future Commercial Transport', 2012, p. 16. cited on page 3

[2] Carrier, G. G., Arnoult, G., Fabbiane, N., Schotte, J.-S., David, C., Defoort, S., Benard, E., and Delavenne, M., 'Multidisciplinary analysis and design of strut-braced wing concept for medium range aircraft', *AIAA SCITECH 2022 Forum*, AIAA SciTech Forum, American Institute of Aeronautics and Astronautics, Dec. 2021.
DOI: 10.2514/6.2022-0726 cited on page 3

[3] Airbus, 'Airbus reveals new zero-emission concept aircraft | Airbus', Oct. 2021.
URL: https://www.airbus.com/en/newsroom/press-releases/2020-09-airbus-reveals-new-zero-emission-concept-aircraft cited on page 3

[4] Belvin, W. K., Doggett, W. R., Watson, J. J., Dorsey, J. T., Warren, J. E., Jones, T. C., Komendera, E. E., Mann, T., and Bowman, L. M., 'In-Space Structural Assembly: Applications and Technology', *3rd AIAA Spacecraft Structures Conference*, AIAA SciTech Forum, American Institute of Aeronautics and Astronautics, Jan. 2016.
DOI: 10.2514/6.2016-2163 cited on page 4

[5] Cheung, K. C. and Gershenfeld, N., 'Reversibly Assembled Cellular Composite Materials', *Science* 341.6151 (Sept. 2013), Publisher: American Association for the Advancement of Science Section: Report, pp. 1219–1221.
DOI: 10.1126/science.1240889 cited on page 4

[6] Costa, A., Jenett, B., Kostitsyna, I., Abdel-Rahman, A., Gershenfeld, N., and Cheung, K., 'Algorithmic Approaches to Reconfigurable Assembly Systems', *arXiv:2008.11925 [cs]* (Aug. 2020), arXiv: 2008.11925.
DOI: 10.1109/AERO.2019.8741572 cited on page 4

[7] Martins, J. and Ning, A., 'Engineering Design Optimization'. Cambridge University Press, 2021.
ISBN: 978-1-108-83341-7 cited on page 15